C-RED one: ultra-high speed wavefront sensing in the infrared made possible

J.L. Gach *[a,b], Philippe Feautrier[a,c], Eric Stadler[a,c], Timothee Greffe[a], Fabien Clop[a], Stéphane Lemarchand[a], Thomas Carmignani[a], David Boutolleau[a], Ian Baker[d]

[a]First Light Imaging S.A.S. 100, Route des houillères, 13590 Meyreuil, France;
[b]Aix Marseille Université, CNRS, LAM (Laboratoire d'Astrophysique de Marseille) UMR 7326, 13388 Marseille, France;
[c]IPAG, Domaine Universitaire, 414 rue de la Piscine, BP 53 38041 Grenoble Cedex 9, France;
[d]SELEX ES, Southampton, Hampshire SO15 OLG, UK

*jeanluc.gach@first-light.fr; phone +33 4 42 61 29 20, www.first-light.fr

ABSTRACT

First Light Imaging's CRED-ONE infrared camera is capable of capturing up to 3500 full frames per second with a subelectron readout noise. This breakthrough has been made possible thanks to the use of an e-APD infrared focal plane array which is a real disruptive technology in imagery. We will show the performances of the camera, its main features and compare them to other high performance wavefront sensing cameras like OCAM2 in the visible and in the infrared. The project leading to this application has received funding from the European Union's Horizon 2020 research and innovation program under grant agreement N° 673944.

Keywords: infrared wavefront sensing, e-apd, infrared camera, high speed, low noise

1. INTRODUCTION

1.1 The C-RED one infrared APD camera

C-RED is a unique commercial infrared camera using the Selex Saphira 320×256 pixels HgCdTe e-APD array with 24 microns pixel pitch. C-RED is developed by First Light Imaging [1]. The sensor cutoff wavelength is 2.5 microns and it allows sub-electron readout noise, taking advantage of the e-APD noise-free multiplication gain and non destructive readout ability. C-RED is also capable of multiple regions of interest (ROI) readout allowing faster image rate (10's of KHz) while maintaining unprecedented sub-electron readout noise.

The sensor is placed in a sealed vacuum environment and cooled down to cryogenic temperature (80K) using an integrated vibration-free pulse tube, with a high reliability (MTBF > 90 000 h) much higher than standard Stirling coolers used usually with cooled infrared arrays.

The Fig. 1 shows a picture of the C-RED one camera prototype. The commercial camera will include a special housing, not shown in this figure, to protect the fragile components of the system and to avoid water condensation inside the camera. On top of the camera, the helium compressor for cooling the pulse tube can be seen on this figure.

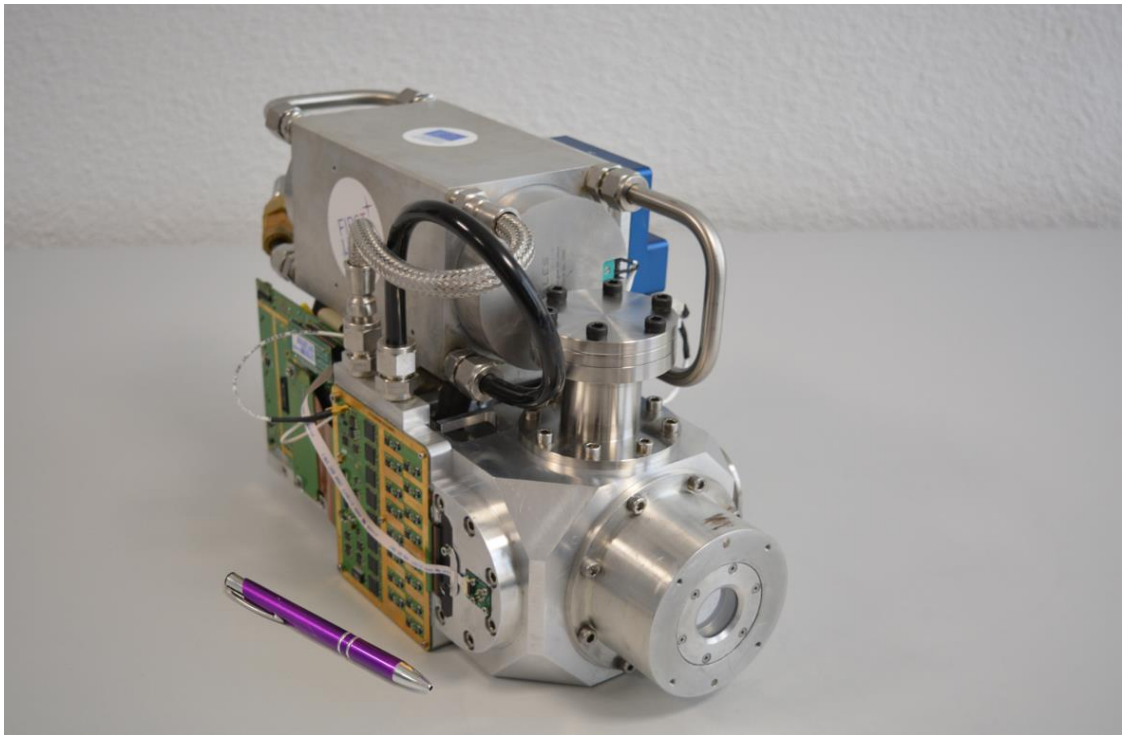

Fig. 1: the C-RED one infrared camera commercialized by First Light Imaging without its outer skin. The pulse tube compressor can be seen on the top whereas in the bottom are the vacuum cryostat and the readout electronics. The purple pen gives the scale.

1.2 The Selex Saphira detector of C-RED one.

Designed and fabricated by Selex, the Saphira detector is designed for high speed infrared applications and is the result of a development program alongside the European Southern Observatory on sensors for astronomical instruments [3]. It delivers world leading photon sensitivity of <1 photon rms with Fowler sampling and high speed non-destructive readout (>10K frame/s). Saphira is an HgCdTe avalanche photodiode (APD) array incorporating a full custom ROIC for applications in the 1 to 2.5µm range.

The SAPHIRA detector uses the HgCdTe APD properties, offering sub-electron noise with multiplication gain up to x400. The pixel format is 320x256 pixels with 15fF integration node capacitance (28fF with HgCdTe diode). The array has 32 parallel video outputs, organized as 32 sequential pixels in row. The 32 outputs are arranged in such a way that the full multiplex advantage is available also for small sub-windows. Non-destructive readout schemes with subpixel sampling are possible. This reduces the readout noise at high APD gain well below the sub-electron level at frame rates of 1 KHz. The growth technology used now is the metal organic vapour phase epitaxy (MOVPE). This growth technology provides more flexibility for the design of diode structures. It is possible to make heterojunctions with different bandgap properties between the absorption region and the multiplication region. The change to MOVPE resulted in a dramatic improvement in the cosmetic quality with 99.97 % operable pixels at an operating temperature of 85K. The avalanche gain is controlled by an external voltage. The digital and analog functions are controlled by a serial interface. The readout of Saphira allows to read multiple windows, each independently resettable. Glow protection and APD protection circuit are also included.

The Fig. 2 shows the functional bloc diagram of the ME911 & ME1000 SAPHIRA readout circuit used currently in C-RED. The ME1000 scanning modes include a Read-Reset-Read per row function, so the user can have complete control of the correlated-double-sampling process. Saphira ME1000 incorporates also glow suppression by using 100% metal screening. A reset current limit function has been added in this readout circuit version to protect the array from short circuit APDs.

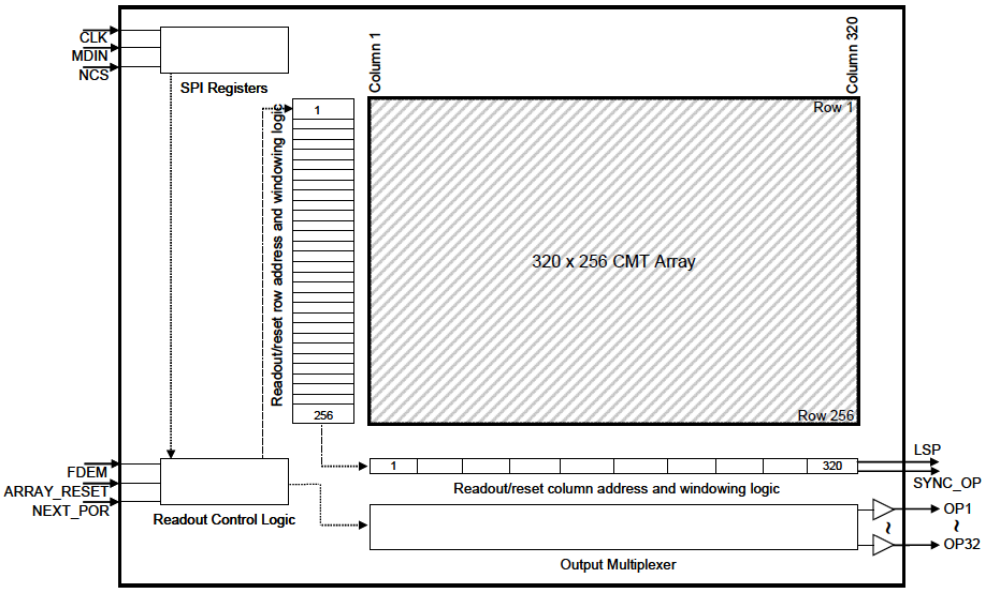

Fig. 2: the SELEX SAPHIRA ME 911/ ME1000 readout circuit architecture.

1.3 The C-RED camera characteristics and performances

The C-RED one camera has the following main characteristics:

- MCT near IR Avalanche Photo Diode 320X256 with Selex Saphira detector.
- Sub-electron readout noise,
- 32 outputs, up to 3500 fps.
- Mean Readout noise at 3500 fps and gain 60 <1 e.
- 70% QE.
- Supported readout modes: read-reset-read per row, embedded multiple non destructive readout, rolling reset
- Pulse tube packaging cooling down to 50 K
- Custom design available (beam aperture)
- Cameralink full interface

1.4 Signal to noise comparison between detector technologies

At various illumination levels, the Signal to Noise-Ratio (SNR) of various visible and infrared detectors is computed by equation (1).

$$SNR = \frac{S}{N} = \frac{QE * S}{\sqrt{QE * S * F + \sigma^2}} \quad (1)$$

In this equation, the detector is assumed to be fast enough to have negligible dark signal. Here, S is the illumination signal (in photons/pixel/image), QE is the detector quantum efficiency, σ is the readout noise, and F is the excess noise factor. A comparison of infrared detectors shows how much an e-APD sensor can improve the SNR for faint fluxes and also that its sensitivity in the infrared is directly comparable to EMCCDs in the visible—the latter of which are considered to be the most sensitive detectors (see Fig. 3).

Currently, the gain in performance of EMCCDs compared to classical CCDs in the visible is smaller than the gap between C-RED One and its competitors— whether they be slow-scan HgCdTe or even indium-gallium-arsenide (InGaAs)-based cameras. This advance in performance characteristics should allow e-APD imagers to usher in a new era in high-performance infrared detection.

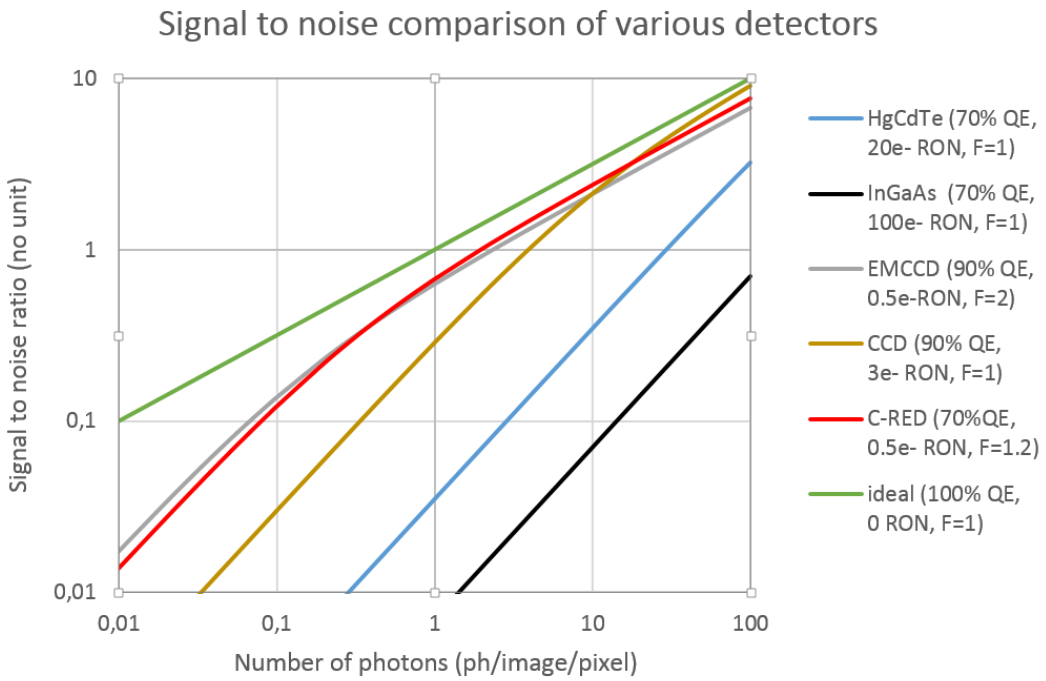

Fig. 3: Signal to Noise comparison of various detector technologies. CCD and EMCCD are sensitive in the visible. They are compared with IR detectors (InGaAs, slow scan HgCdTe and the C-RED e-APD camera).

2. MEASURED C-RED ONE PERFORMANCES

The measurements were all made at 80K operating temperature, using a MARK 13 engineering grade SAPHIRA device. This device is supposed working as a science grade except for cosmetics which should be degraded.

2.1 Quantum efficiency

The array quantum efficiency peaks up to near 80% and the array AR coating may be optimized on a per-device basis for J, H or K bands. Fig. 4 shows the effect of this QE optimization. Moreover due to junction heterostructure with 3.5µm cutoff wavelength HgCdTe material for the avalanche multiplication region and 2.5 µm material for the absorber, the device is sensitive in L band at gain 1 but not with APD gain. This is due to photon penetration depth (longer wavelength photons penetrate deeper in the material and therefore are less amplified). We've measured that already with low gains (in the range of 5 to 10) the L band sensitivity is decreased to near zero, leaving only J, H and K sensitivity.

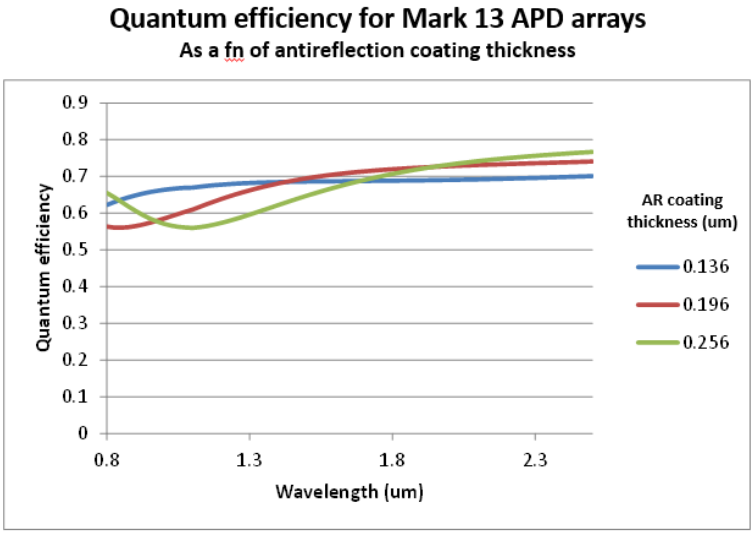

Fig. 4: AR coating and QE optimization for J, H or K bands of Mark13 e-APD diodes.

2.2 System gain

The system gain is measured illuminating the sensor with a flat field through an integrating sphere. Then temporal noise versus illumination level is plotted in log/log scale to have the system gain and the noise level (see Fig. 5). The system gain in an infrared device depends strongly upon the diode polarization. Indeed the diode capacitance is used to integrate the charges and its value depends on the reverse voltage applied (the higher, the lower is the diode capacitance). For a 2V reverse bias, which corresponds to a gain of 1, the system gain was measured at 1.1e^-/ADU which is in perfect accordance with the expected 1.15 e^-/ADUsystem gain with a 28fF node capacitance.

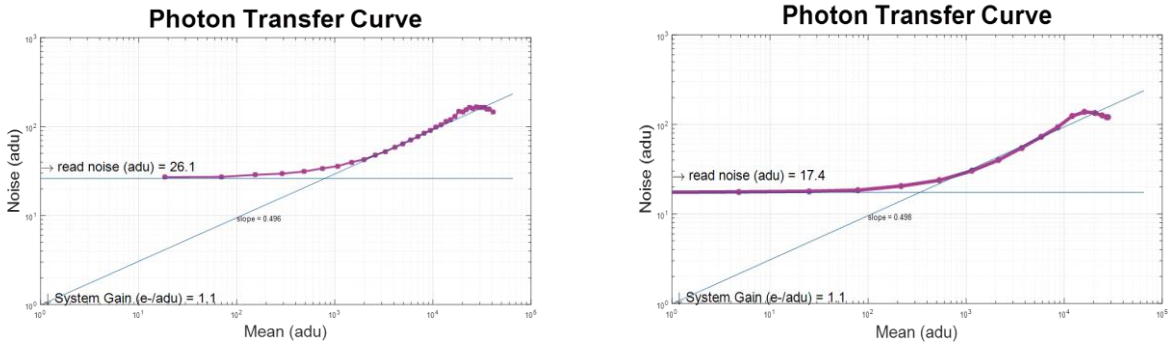

Fig. 5: Photon transfer curve of single readout mode (left) and CDS mode (right).

2.3 APD gain

APD gain is measured by illuminating the sensor with a weak light, apply APD gain, and measure the ADU change. To get rid from any FPN, the level measurement is done by subtracting images at 50FPS and 25FPS. Fig. 6 shows that APD gain vs bias voltage and the exponential fit. The gain can be expressed as $G=0.4121e^{0.3548Vbias}$ which is in accordance with other measurements carried out by various groups using these devices.

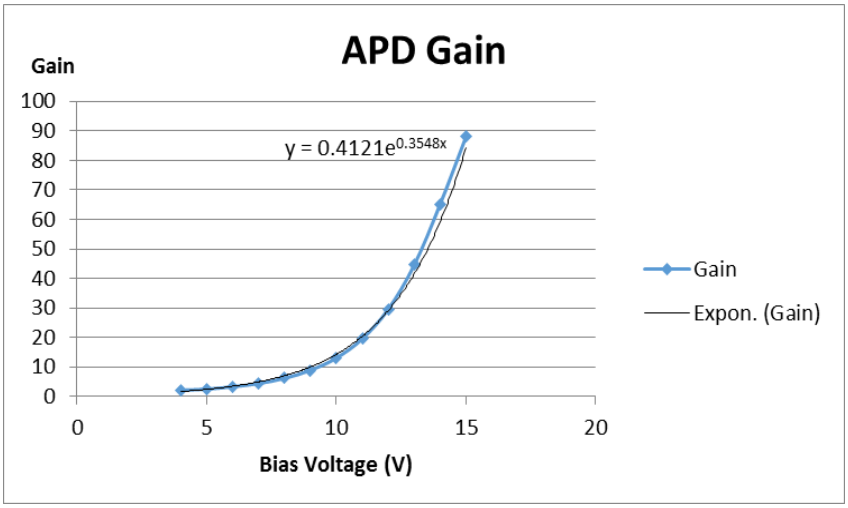

Fig. 6: Measured APD gain vs polarization voltage of MARK 13 array and exponential fit.

2.4 System noise

The noise measurement is done by measuring the temporal variation of the image, sensor in the dark looking at a 80K blackbody. Measurements have been done for single readout and CDS readout. Taking into account 28fF node capacitance, the KTC noise should be in the range of 35e- at 80K. Fig. 7 shows the sensor readout noise in single readout and CDS readout modes. It can be noticed that the CDS mode reduces the readout noise by the KTC noise at the expense of a supplementary readout, hence a reduction in the maximal frame rate by a factor of two. It might be noticed that the noise scales perfectly with APD gain, therefore increasing APD gain does not increase readout noise as it should be expected. Finally it can be noticed also that for gains > 30, the array enters in subelectron readout whatever is the readout mode (single readout or CDS). This is really a change of paradigm in the way of operating infrared arrays since CDS is no more needed to minimize readout noise, simply by increasing the APD gain, one can have very low noise operation, without compromise on readout speed, but at the expanse of a lower dynamic range (typically 30% less dynamic range in our case).

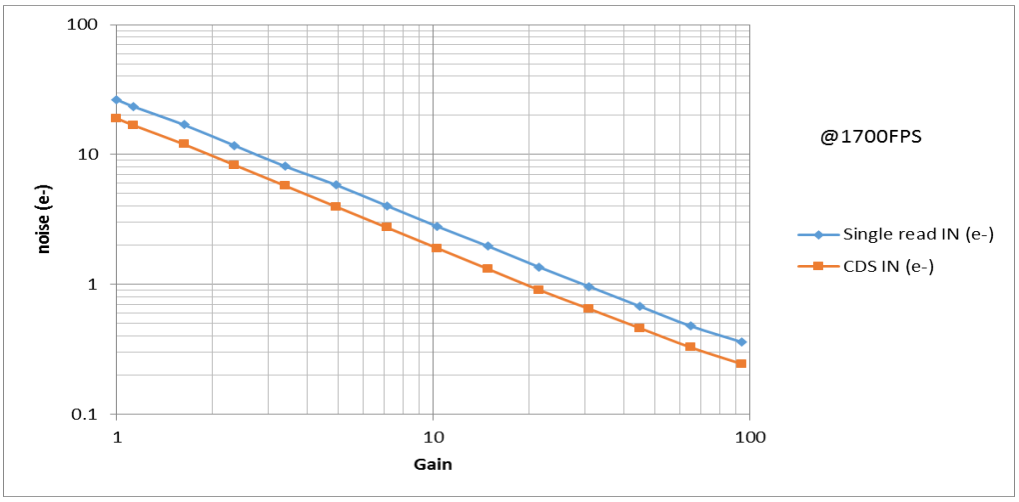

Fig. 7: Measured input referred readout noise vs APD gain for single readout and CDS readout.

2.5 Dark current

To do this measurement the sensor is in the dark, looking at a 80K blackbody.The dark current is measured by fitting a line over the ADU level vs exposure time graph. The slope of this line gives the mean dark count in ADU/s. The

operation is repeated for several gains. The result is plotted in Fig. 8. The mean system dark is in the range of 80 e^-/s/pixel. According to Selex data, the dark current should be rather in the range of 20 to 50e^-/s/pixel. The difference is suspected to be some weak photons leakage of the cold cryostat. The evidence is that the dark is increased for low and high gains. At low gains the sensor is sensitive up to 3.5 um, therefore more sensitive to photon lekeage, whereas at high gains the dark current should be limited by trap assisted tunneling which is in the range of 100e^-/s/pixel at a gain of 100, in accordance with our measurement. Even if it is not really limiting, the source of this weak leakage has been identified and will be fixed in production versions.

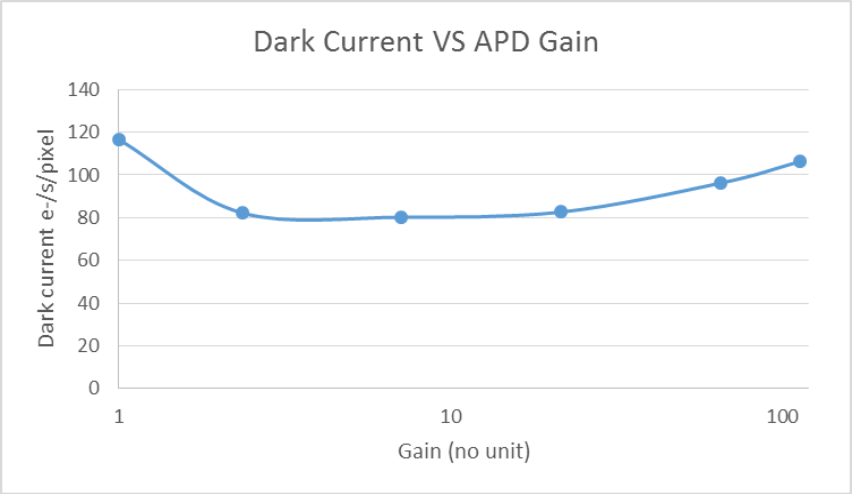

Fig. 8: Measured dark current vs APD gain.

2.6 Cosmetics

One of the advantage of this sensor is its extremely good cosmetics, even when high gain is applied. Some other groups reported only a few dead pixels over the entire array, which is due to the HgCdTe growing process (MOVPE). Even with our engineering grade device, the cosmetics was excellent only showing a few pixels with leakage dark current (see Fig. 9). Shows images at various gains. Again this device changes the paradigm of infrared FPA use since we have a cosmetics comparable to a CCD, or even better with nearly zero defect. This device is really operated like an EMCCD, and people already familiar with these latter ones will notice almost the same behavior except that unlike EMCCDs, e-APDs are not sensitive to overillumination. The red and grey curves of Fig. 3 perfectly illustrate this common behavior.

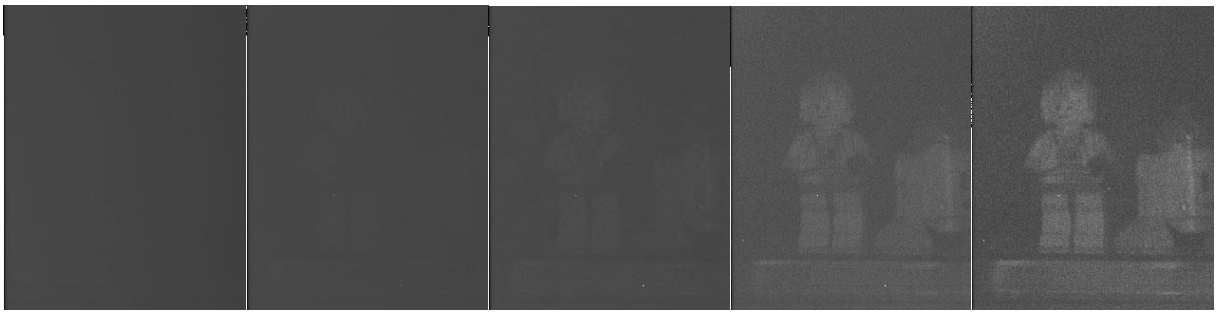

Fig. 9: Low light scene imaged with gains of 1,6,13,45 and 90 (from left to right) showing only a few defective pixels at high gain (<10 defective pixels) on our engineering grade device, CDS readout at 1700 FPS.

2.7 Cropping

C-Red allows multiple region of interest readout (MROI).The sensor uses 32 output amplifiers in parallel therefore is virtually split in a square of 10 columns of 32 pixels and 256 rows. It is then possible to select one or more sub region by

selecting any column and row number. Fig. 10 illustrates the MROI readout mode. The output geometry of the frame will always be rectangular. In this mode the maximal frame rate scales with the number of pixels read out, therefore extremely high frame rates may be used, even when using CDS or multiple readout.

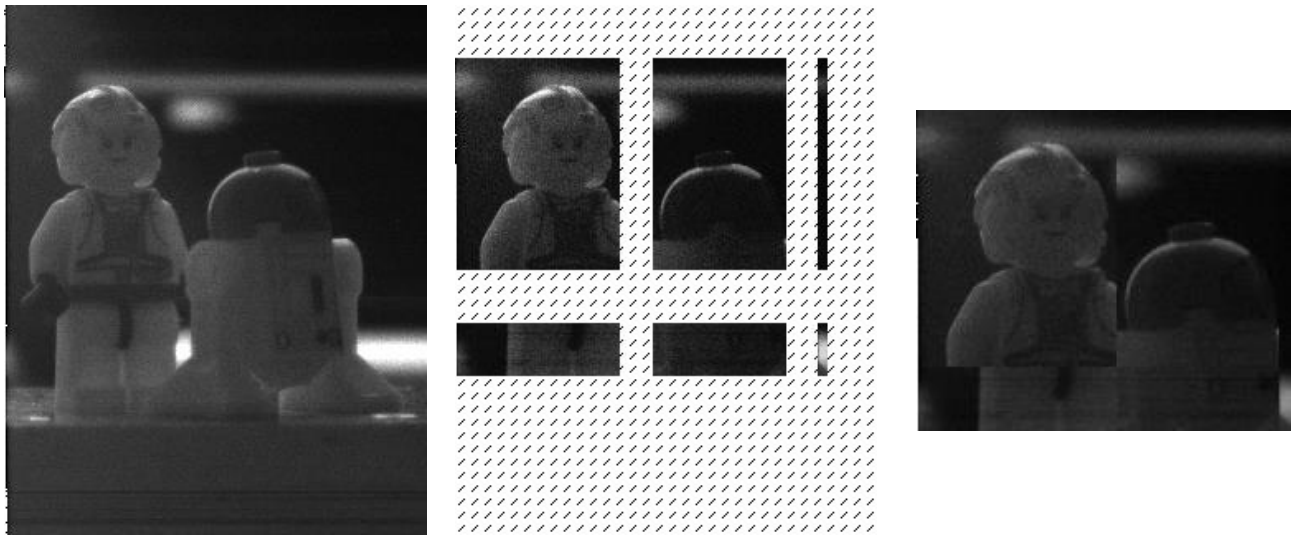

Full Frame ReadOut. 1700FPS *6 different regions. 3400FPS* *Raw Frame as sent by C-Red One.*

Fig. 10: Example of a cropping on Global Reset Mode with Correlated Double Sampling. The maximum frame rate increase with a reduction of the image size.

3. OPERATION

3.1 Background issues

The major issue with such a camera is not to kill the performance with a high thermal background. Indeed a 300K blackbody has already a strong emission in the K band regarding the readout noise and the dark current of the sensor itself. Moreover, the L band sensitivity at low gain will amplify the background contribution, therefore it is mandatory to filter out these wavelengths. C-RED one uses a proprietary cold filter set that can be adjusted at will to minimize the unwanted background. Therefore J and H bands are accessible with hot optics, without any particular precaution. Working in the K band will require cold optics, and K short might be accessible with moderately cooled optics. Fig. 11 shows the simulated integral contribution of the background with the standard H and K filter set, when the camera is looking at a blackbody at 300K. Of course this is a worst case example since the actual instrumentation should have an emissivity in the range of 5%. The simulation has been done for a gain of 1, where the sensitivity of the sensor in L band is maximal, again in the worst case. The actual measured blackbody background in 0.8 e^-/ms/pixel at a gain of 1 and 0.4 e^-/ms/pixel at a gain of 20, very close to the cryostat background itself. The slight discrepancy of the simulation vs actual data is mainly due to the overestimation of the L band sensitivity of the device and especially the real cutoff wavelength around 3.5µm where should be the major background contribution. Finally the actual input referred background is lower at higher gain due to L band sensitivity decrease with gain.

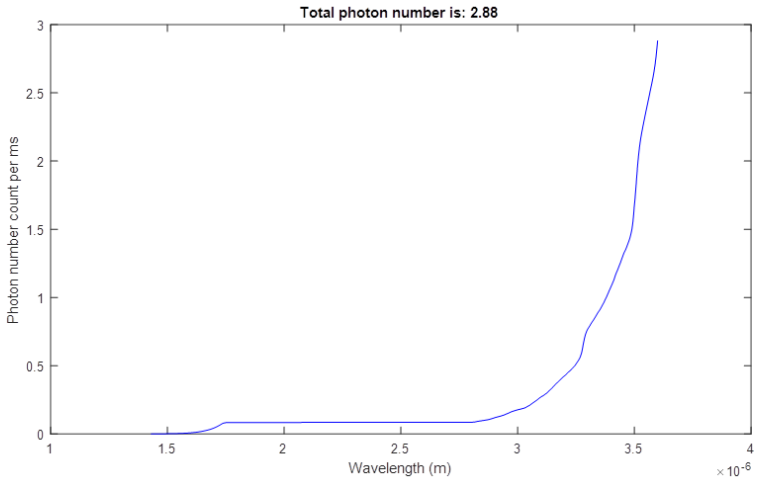

Fig. 11: cumulative integral background contribution in e^-/ms/pixel for a 300K blackbody scene.

3.2 Use of integrated cold optics

The use of a 4W cold power pulse tube permits the integration of cold optics inside the camera cryostat, at will, using part of the cooling power margin to cool down for example a microlens array or a collimator lens for a pyramid wavefront sensor. Depending on the used wavelengths, several configurations are possible with cold, partially cooled or hot optics. The camera may also be interfaced to a third party cryostat enclosing cold optics with shared vacuum to minimize background and to have access to the full K band. Fig. 12 shows the inner cold shield assembly with the beam entrance, optics can be inserted at this level with minor modifications.

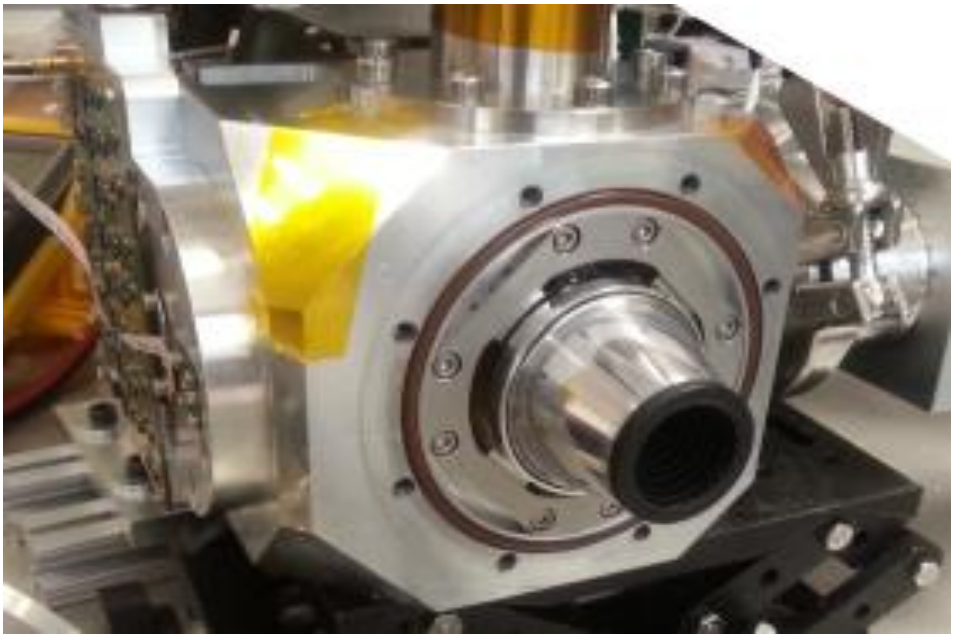

Fig. 12: The inner cold shield view with the beam entrance, where cold optics may be inserted for K band operation. J and H bands operation can use warm optics thanks to the cold filter assembly (not visible here).

4. CONCLUSION

We've demonstrated the ability of CRED-ONE to have comparable or even better performance than visible fast cameras dedicated to AO wavefront sensing like OCAM2 : this camera offers fast frame rate, subelectron noise, low background, wide spectral response over J, H and K bands, and outstanding cosmetics compared to other SWIR cameras. It has been demonstrated that there is a strong theoretical advantage to use e-APDs for NGS on large telescopes (see [4]), and e-APD technology is now mature enough to be used in wavefront sensing. C-RED one permits then a significant advance in short wave infrared imaging and is opening new windows for wavefront sensing.

REFERENCES

[1] P. Feautrier et al., "OCam with CCD220, the Fastest and Most Sensitive Camera to Date for AO Wavefront Sensing", Publ. Astron. Soc. Pac. Vol 123 n°901, 263-274 (2011)

[2] J.L. Gach and P. Feautrier, "Electron initiated APDs improve high-speed SWIR imaging", Laser Focus World vol 51 n°9, 37-39, (2015)

[3] G. finger et al., "Evaluation and optimization of NIR HgCdTe avalanche photodiode arrays for adaptive optics and interferometry", Proc. SPIE 8453, 84530T (2012).

[4] Feautrier, Philippe, Gach, Jean-Luc, Wizinowich, Peter, "State of the art IR cameras for wavefront sensing using e-APD MCT arrays", AO4ELT4 Conference, 2015.